Quaternary Research 75 (2011) 347–355

Contents lists available at ScienceDirect

Quaternary Research

journal homepage: www.elsevier.com/locate/yqres

Micro-relief development in polygonal patterned ground in the Dry Valleys of Antarctica

Bernard Hallet *, Ron Sletten, Kevin Whilden

Quaternary Research Center and Department of Earth & Space Sciences, University of Washington, Box 351310, Seattle, WA 98195-1310, USA

ARTICLE INFO

Article history:
Received 19 February 2010
Available online 18 February 2011

Keywords:
Periglacial features
Patterned ground
Permafrost
Mars
Europa
Planetary

ABSTRACT

Polygonal patterned ground in polar regions of both Earth and Mars has received considerable attention. In comparison with the size, shape, and arrangement of the polygons, the diverse micro-relief and topography (termed here simply "relief") of polygonal patterned ground have been understudied. And yet, the relief reflects important conditions and processes occurring directly below the ground surface, and it can be observed readily in the field and through remote sensing. Herein, we describe the relief characteristic of the simplest and relatively young form of patterned ground in the Dry Valleys of Antarctic. We also develop a numerical model to examine the generation of relief due to subsurface material being shouldered aside contraction cracks by incremental sand wedges growth, and to down-slope creep of loose granular material on the surface. We model the longterm subsurface deformation of ice-cemented permafrost as a non-linear viscous material. Our modeling is guided and validated using decades of field measurements of surface displacements of the permafrost and relief. This work has implications for assessing the activity of surfaces on Earth and Mars, and much larger scale potential manifestations of incremental wedging in icy material, namely the distinct paired ridges on Europa.

© 2011 University of Washington. Published by Elsevier Inc. All rights reserved.

Introduction

Polygonal patterned ground is one of the most distinctive landforms in permafrost terrain of the polar regions (Fig. 1), and of the permafrost planet, Mars. A multitude of recent high-resolution images of Mars and close ups from the Phoenix lander is revealing, with striking clarity, a diversity of patterned ground that varies considerably in terms of size, shape, regularity, relief, and organization of boulders (e.g., Mellon, 1997; Mellon et al., 2008, 2009; Lefort et al., 2009; Levy et al., 2009a,b). As these diverse forms of patterned ground appear to have much in common with patterned ground on Earth, there is considerable motivation to seek better understanding of the terrestrial analogs.

The planform of decameter-scale polygonal patterned ground is initially established by the propagation and mechanical interaction of thermal contraction cracks. Cracks form when tensile stresses induced by the cooling of the ground surface and subsurface exceed the tensile strength of the frozen soil (Lachenbruch, 1962, 1963; Pewe, 1974). Prior to fracture, thermal contraction while the permafrost is cooling induces primarily tensile stress parallel to the ground surface. Formation of a fracture abruptly relieves the stress in the vicinity of the fracture. Fracture propagation and intersection ultimately result in a polygonal network of vertical or near-vertical cracks penetrating from the surface to depth. On Earth, they typically penetrate several meters below the surface and are spaced a few meters to several tens of meters apart.

In a seminal paper, Lachenbruch (1962) calculated the tensile stress that develops in thermally contracting permafrost. He treated the ice-cemented soil as a Maxwellian viscoelastic solid, which on short time scales responds to thermal contraction by an elastic buildup of stress, and that relaxes viscously on longer time scales. He calculated the tensile stress that could be maintained for a constant cooling rate and rheological properties of ice near 0°C. He found that tensile stresses could reach values exceeding the tensile strength of frozen soil for reasonably high cooling rates, consistent with observations of cracking in the Arctic.

Mellon (1997) developed a model to examine the formation of thermal contraction cracks on Mars. The model treats the ice-rich permafrost as a semi-infinite, isotropic half-space with a time-dependent vertical temperature distribution consistent with seasonal variation in surface temperature. The model uses rheological data of ice (e.g., Hobbs, 1974; Weertman, 1983; Kirby et al., 1987) and frozen ground (e.g., Tsytovich, 1975; Andersland et al., 1978; Durham et al., 1992) not available to Lachenbruch (1962) and considers the thermoelastic stresses arising from a soil thermal regime appropriate for Mars. These models are robust tools that shed quantitative light on the size of polygons and their dependence on the depth of contraction cracks, which is a function of the temperature forcing and the rheological properties of permafrost.

Thermal contraction cracks tend to open at the ground surface during cold periods, and in arid regions they tend to fill partially with

* Corresponding author. Fax: +1 206 543 0489.
E-mail address: hallet@u.washington.edu (B. Hallet).

0033-5894/$ – see front matter © 2011 University of Washington. Published by Elsevier Inc. All rights reserved.
doi:10.1016/j.yqres.2010.12.009

https://doi.org/10.1016/j.yqres.2010.12.009 Published online by Cambridge University Press



Figure 1. Victoria Valley polygons showing raised shoulders on of polygonal patterned ground with typical dimensions of about 20 m.

sand and other fine-grained debris. This infilling prevents the cracks from closing fully during warm periods. Crack-normal horizontal compressive stresses arise during the warming phase, producing deformation and uplift along the crack (Fig. 2). With time, the ground surface on both sides of the crack is warped upward to form symmetrical ridges separated by a trough over the crack. During subsequent cooling periods, the crack reopens, permitting more sand that ravels down the slopes of the trough to fall into the crack, thereby incrementally forming a wedge of sand. The recurrent expansion, infilling, contraction cycles result in continued growth of shoulders surrounding the cracks.

Similar relief also occurs in cold regions with more abundant moisture. In these regions, ice-wedge polygons form as snow melts or ice-rich frozen ground thaws at the surface during the warming phase, thereby filling cracks that penetrate into the frozen ground with water, which subsequently freezes to form ice wedges. Compared to sand-wedge polygons, ice-wedge polygons have received considerable attention. Notably, they have been the subject of an extensive series of field studies conducted or led by Ross Mackay (1971, 1974, 1984, 1986, 1992, 1993, 2000; Mackay and Burn, 2002). More recently, extensive numerical studies have addressed the self-organized development of polygonal patterned ground, the resulting plan form geometry, and the dependence of the morphology of the polygons and size of the wedges on evolving climatic conditions (Plug and Werner, 1998, 2001, 2002, 2008). Specific aspects of these studies have generated significant controversy (Burn, 2004).

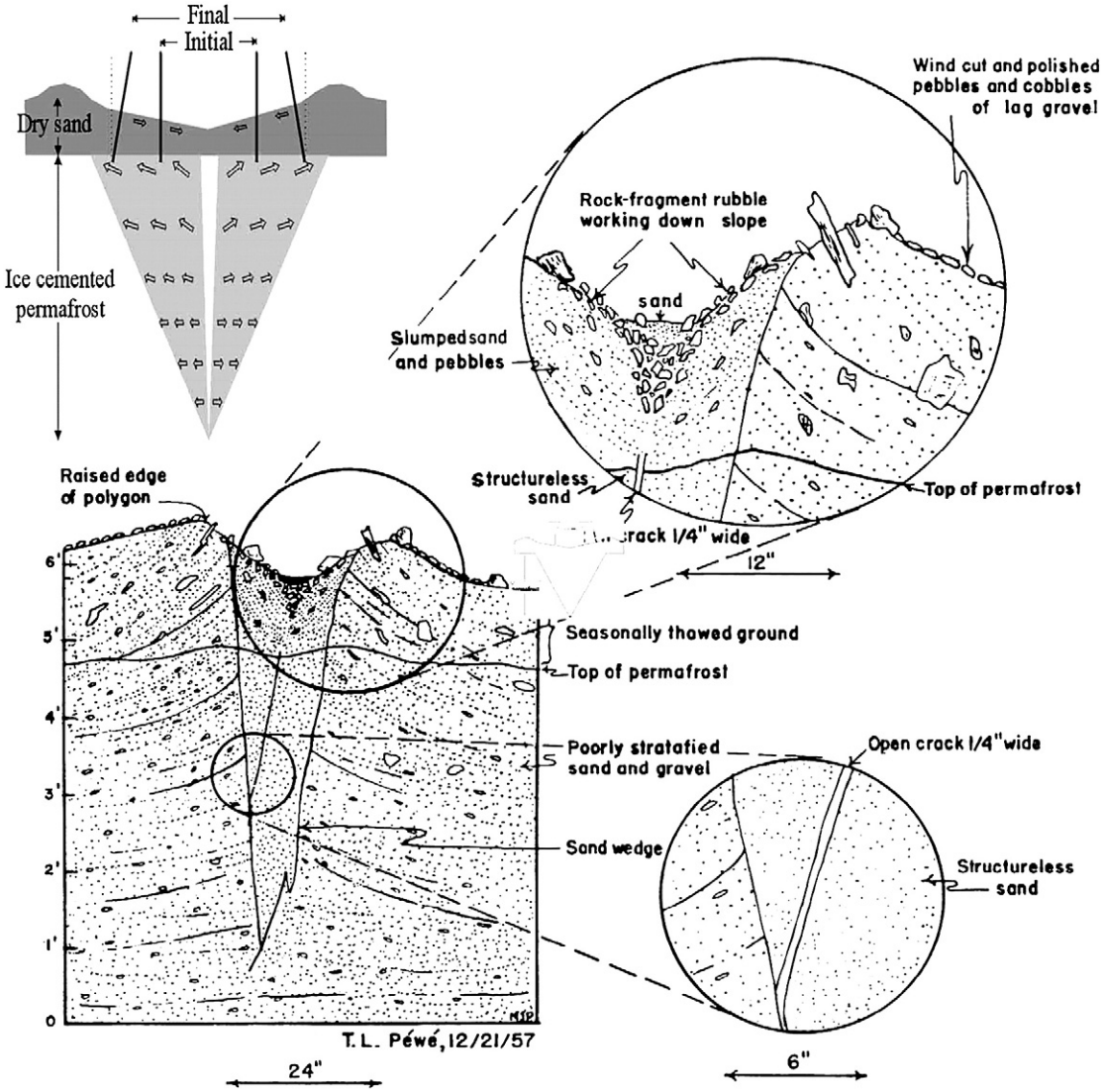


Figure 2. Subsurface deformation due to growth of sand wedges, modified from sketch by Troy Pewe (1959) with added inset in the upper left to represent the measurements of wedge growth initiated by Black and Berg (1963) using pairs of vertical rods across contraction cracks; the rods diverge progressively with time.

https://doi.org/10.1016/j.yqres.2010.12.009 Published online by Cambridge University Press

Our focus

Herein, we examine the development of relief, which is conspicuous but has received comparatively little attention. This relief and the corresponding long-term deformation of the upper few meters of permafrost result from the slow growth of sand or ice wedges over thousands of years. This deformation, and in particular the shouldering aside of material adjacent to the wedges, are required due to the recurrent addition of material in steeply dipping cracks that open periodically due to surface-parallel tensile thermal stresses. We emphasize that this permanent deformation is quite distinct from the periodic, cyclic deformation that results directly from the thermal cycling but produces little or no net permanent surface deformation. Moreover, the permanent deformation we focus on is primarily a function of the amount of material that is added to open cracks, and that is independent of the cyclic thermally induced strains except for their role in opening cracks that allow for an external input of material into the cracks.

We hope that the work presented here will constitute a first step in examining how the surface relief reflects significant subsurface processes that cannot be studied using remote sensing, and that are generally rather elusive, especially on Mars or other remote environments. These processes include thermal contraction and expansion, fracture, crack infilling, long-term permafrost deformation, and sublimation of subsurface ice. Our work may also help understand the long-term deformation of permafrost surrounding growing wedges that is clearly evident in practically all exposure of ice wedges (e.g., Washburn, 1973; Jahns, 1975), and that has been examined quantitatively in the field by Mackay (2000), Mackay and Burn (2002) and Matsuoka (2011).

Diverse types of polygonal patterned ground relief occur in the Dry Valleys and also are seen in other regions on Earth and Mars. They most likely reflect different histories of wedge activity and distinct substrates. We stress that this diversity of relief is not addressed explicitly here, though many of the processes we discuss pertain to these other terrains. A number of ideas have emerged to account for the range of mature polygon forms and relief in the Dry Valleys (see Bockheim et al., 2009, and references therein); they have led to diverse and instructive conceptual models. These contrast with our model, which is quantitative but addresses only the early stages of polygon relief development for a simple, idealized system.

Our research is guided by observations of the relief and over 45 yr of growth measurements initiated by Robert F. Black (Black and Berg, 1963; Black, 1973) on sand wedges in the Dry Valleys of Antarctica. We use these measurements as input to a model of long-term polygon deformation coupled with a surface creep model that is focused on the generation of the slopes immediately adjacent to the polygon cracks. These models provide insight into the character, magnitude and spatial extent of material deformation within an entire polygon in response to wedge growth. It also shows how the surface relief reflects the wedge shape, rheology of the permafrost and the vigor of sand-wedge growth and incremental wedging.

For assessing the model results we focus on topographic profiles transverse to ridges along the perimeter of representative sand-wedge polygons in Upper Victoria Valley, because the polygons in this area have developed relatively recently on a former delta in a lake that extended over much of the valley floor. According to Kelly et al. (2002), the surface is estimated to be slightly younger than 12,000 yr based on ^{14}C dating of algal deposits. Such a surface is ideal because the initial surface form and composition are known; the initial surface can be assumed with confidence to be essentially planar, and the sediment substrate is relatively homogeneous. Moreover, the age of the surface can be constrained, and the layering in the sediment permits definition of the subsurface deformation, which could also be modeled with the approach taken here but is beyond the scope of this paper.

Modeling description, assumptions and validation

We assume that all but the upper few decimeters of frozen sediment acts as a continuum. This material is ice-cemented permafrost with considerable variation in ice content and texture. Our shallow excavations and those of others (Pewe, 1959; Black and Berg, 1963; Black, 1973) reveal that the surface is often underlain by fine-grained sand cemented with ice. Farther down the permafrost is generally saturated or supersaturated with ice in many Dry Valley sites. Even where large (1–3 m diameter) boulders cover much of the surface, as in lower Beacon Valley, well-sorted sand is dominant directly below the surface. We explore the development of the relief using two models that are coupled: a finite-element model to examine the subsurface deformation of the permafrost and a granular-creep model to study the surficial "raveling" of loose sand into the contraction cracks and the evolution of the steep converging slopes that form the trough centered above these cracks.

Permafrost deformation model

We used a commercial finite element (FE) package noted for its ability to model non-linear visco-elastic solids (ABAQUS v5.8), and we created a 2D model to simulate the material deformation in response to long-term incremental wedge growth with a focus on the resulting long-term development of the characteristic relief of polygonal patterned ground. The model used the rheological properties of ice because the rheology of frozen soils is often approximated with that of ice (e.g., Mellon, 1997), and considerably more experimental data exist for ice than for frozen ice–soil mixtures. This is a reasonable assumption since our field observations have shown that Dry Valley polygon material is typically fine-grained ice-cemented sand, where permafrost deformation is likely dominated by the viscous behavior of the ice. The model uses Glen's Flow Law to relate strain rates, $\dot{\varepsilon}_{ij}$, to deviatoric stresses, σ'_{ij}, the effective shear stress τ_e, and material constants A and n, which are known through various laboratory studies (e.g., Cuffey and Paterson, 2010):

$$\dot{\varepsilon}_{ij} = A\tau_e^{n-1}\sigma'_{ij}. \quad (1)$$

We tested the results produced by ABAQUS by comparing them to a well-known analytical solution for a non-linear viscous material model. The state of stress in an infinite viscous fluid around an open cylindrical tunnel (Nye, 1953), as a function of tunnel radius and distance from the tunnel wall, provides a strong indication of whether the model properly handles the non-linear rheology. In this sense, this analytical solution is particularly diagnostic because the anomaly in circumferential stress in the ice ($\sigma_{\theta\theta}$) depends sensitively on the value of the exponent, n, in Glen's Flow Law. It actually switches sign, from compression for $n=1$ to tension for $n=3$; for $n=2$, $\sigma_{\theta\theta}=0$. When tested in this manner, the model adequately reproduced the predicted stress for all values of n.

The model is driven by assigning horizontal displacement rates for the vertical polygon edges that are consistent with sand-wedge growth in the cracks bounding the polygon. Because of this kinematic boundary condition, the choice of temperature, and hence effective viscosity or flow law parameter, A, has relatively little effect on the displacement field and micro-relief, albeit it strongly impacts the stresses. For simplicity, to generate the results presented here we used a single value of A, corresponding to a typical mean surface temperature for the Dry Valleys. The FE calculations used $6.8\times10^{-26}\ s^{-1}\ Pa^{-3}$ for A, the value recommended by Cuffey and Paterson (2010) for $-25°C$. Though rather extreme, this simplification is acceptable for this first step in computing the geometry of permafrost deformation and the shouldering of the polygon borders. We emphasize here that, although they are central to the seasonal and higher frequency

https://doi.org/10.1016/j.yqres.2010.12.009 Published online by Cambridge University Press

variations in stresses and strains in permafrost, we assume for simplicity that thermal driving forces produce only cyclic deformation, and that only the subsurface accumulation of sand forming wedges contributes to net long-term displacements and development of significant relief.

A single polygon is viewed as composed of axi-symmetric elements (Fig. 3) consistent with the symmetry of an idealized polygon. The calculations focus on one such element that represents a vertical slice across a polygon, with one edge located at the center of the polygon and the other edge located at the perimeter. The latter edge is the location of cracking and progressive wedge growth; consequently, the deformation of the entire polygon is driven by the rate of horizontal motion imposed at this edge. This deformation in a vertical plane radial to the polygon center is modeled using a rectangular 2D mesh and assuming plane strain (Fig. 3).

The pattern of deformation of material depends on the variation with depth of the horizontal velocity boundary condition imposed along the crack edge of the model, and the frozen material rheology. From the triangular shape typical of wedges seen in exposures elsewhere, and from a few exposures in the Dry Valleys that show a distinct taper with depth (e.g., Pewe, 1959, and Fig. 2), we infer that long-term horizontal displacements decrease linearly from a maximum value at the top of the crack to zero at the bottom of the crack. This is termed the "tapered velocity" boundary condition and is the simplest way to approximate the most commonly observed wedge shape. The field data that we collected from Black's sites provide a measure of the long-term rate of horizontal displacement of the permafrost at the surface. For comparison, we also ran the model with a uniform horizontal velocity boundary condition (no depth variation).

The velocity boundary conditions and body forces complete the model's representation of a polygon. The top edge of the mesh represents the ground surface; it is treated as traction-free surface where velocities are not constrained horizontally (x direction) or vertically (y direction). Nodes along the vertical edge of the 2D mesh at the center of the polygon are fixed horizontally because of symmetry with respect to the crack occurring on opposite sides of a polygon, but they are allowed to move freely in a vertical direction thereby allowing the ground surface to rise as material is added at depth to the crack edge. The bottom edge of the 2D mesh is fixed in both x and x directions, representing no displacement below the crack depth. The other vertical edge of the mesh represents the contraction crack at the polygon perimeter where the horizontal velocity field is imposed; nodes there are free to move in the y-direction. Gravity is used as a body force for all elements and the permafrost is assumed incompressible. Although gravitational forces are insignificant compared to the viscous forces on the scale of polygons, they are included in the model because they could become important for larger scale relief such as the paired ridges on Europa, which are discussed briefly at the end of this paper. Finally, even though we are interested in permafrost displacements over periods on the order of 10^2–10^5 yr, we focus on the modeled displacement field that results for a single increment that may occur each year, as this repetitive motion suffices to define the pattern of incremental permafrost deformation and subsequent relief development.

Granular creep model

The shallow raveling of sand that lacks the ice cement seems to dominate the relief evolution along the steep slopes bordering the cracks, and up to the crest of the raised shoulders (e.g., Bockheim et al., 2009). This down-slope creep of loose sand in a thin layer, perhaps one or a few particles thick, is addressed in a separate model guided by the results of experimental studies of the surficial motion of sand and the resulting slopes for sand piles (Roering et al., 2001). The slopes observed experimentally closely resemble the slopes adjacent to contraction cracks that delineate polygons (Fig. 4), suggesting that the experimental results have considerable relevance.

In Roering et al.'s (2001) experiments, steady vibration causes a thin layer of sand grains along the sand pile surface to dilate and creep downslope, while the underlying grains remain static. On gentle slopes, sediment transport is driven by local grain dilation and downslope creep. For low surface gradients ($S = 0.16$), the sand flux, q, is fairly uniform in time. "The thin layer of mobile grains resembles a flowing carpet, moving steadily over the entire hillslope. As gradient increases, fluxes become more variable" and erratic, taking on the character of "landslides of variable size and duration." Roering et al. (2001) modeled the evolving shape of their sand piles well with a simple, transport law describing the sand flux as a non-linear function of the surface gradient:

$$q = \frac{KS}{1-(S/S_c)^2} \tag{2}$$

where K is a transport coefficient ($m^2 yr^{-1}$) and S_c is a critical surface gradient resembling the angle of repose.

The evolution of the relief for active sand-wedge polygons can be modeled by combining the rate of surface uplift, $u(x)$, due to the shouldering of material aside growing wedges as calculated with the

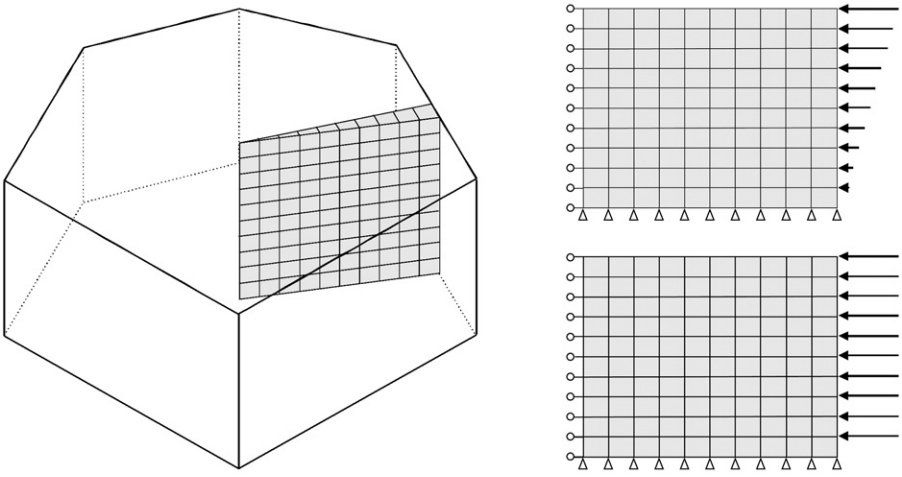


Figure 3. Model geometry and boundary conditions. Left, 3-D perspective diagram showing the cylindrical symmetry of an idealized polygon and vertical slice used for the computation. Right, both types of imposed velocity boundary conditions: horizontal velocity decreasing linearly with depth (upper) and uniform (lower).

https://doi.org/10.1016/j.yqres.2010.12.009 Published online by Cambridge University Press

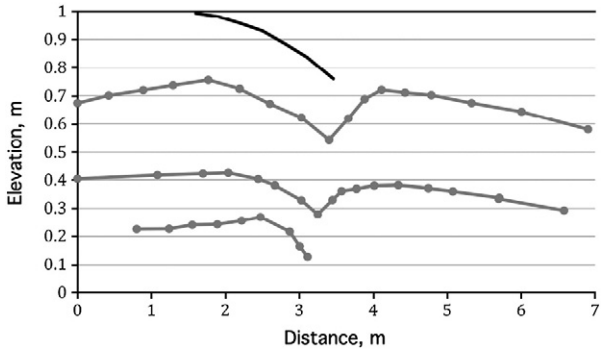


Figure 4. Measured topographic profiles across three polygon boundaries, Victoria Valley, and across one side of a vibrated sand pile (upper line without symbols) as reported by Roering et al. (2001).

finite element model, with the subsidence of the surface due to the divergence of the flux of loose sand at the surface.

$$\frac{\partial z}{\partial t} = u(x) - \frac{\partial q}{\partial x} \tag{3}$$

The flux, q, is given in Eq. (2) in which S varies with x. For convenience, $u(x)$is approximated closely as a simple polynomial fit of the vertical velocity field at the surface calculated by the finite element (FE) model of permafrost deformation:

$$u(x) = u_o\left(0.0053x^2 - 0.089x + 0.455\right) \tag{4}$$

where u_o is a scaling factor for the velocity and x in meters. For the modest relief generated and small permafrost strains involved in the simulations presented below, $u(x)$is treated as being constant in time and independent of the surface creep. The surface creep model, on the other hand, is coupled to the permafrost deformation model through Eq. (3); at each time step of the model the elevation of the surface is updated to reflect both the divergence in the flux of creeping material and uplift of the surface due to the incremental shouldering and permafrost deformation.

Modeling results

The FE model yields a quantitative description of the pattern of permafrost deformation. Fig. 5 illustrates the velocity field through one half of a 20-m-diameter polygon; these vertical cross-sections are 10 m wide and 5 m high, and extend from the polygon center on the left to the growing sand wedge on the polygon periphery. Both the magnitude and orientation of the velocities are shown for two values of the flow law exponent, n, and for the two distinct scenarios for the horizontal velocity field imposed along the polygon crack: the tapered and the uniform velocity boundary conditions.

Significant displacement occurs near the crack, but some displacement occurs throughout the section modeled to depths of several meters where material is added along the contraction crack. For the tapered velocity boundary condition, which most closely mimics the displacement field consistent with the growth of a wedge of sand (or ice), most of the deformation occurs near the crack and the surface, but deformation is significant throughout about 2/3 of the volume of the cross-section, and most of this displacement occurs near the surface. Fig. 5 shows that deformation field depends sensitively on the velocity field imposed at the polygon edge as a boundary condition, and much less so on the rheology.

The FE model results and the choices of rheology and boundary conditions can be assessed by comparing the computed vertical deformation at the surface to measured profiles of polygon shoulders in the polygon interior where the surface is not confounded by material raveling into cracks. Fig. 6 presents surface profiles of vertical displacements for a single time increment calculated for various model scenarios, as well as a profile of polygon relief we measured in Victoria Valley. As we wish to determine which model yields the most realistic pattern of displacements rather than absolute values, the model result were scaled uniformly for all runs to produce relief comparable to the field measurements. The best match to the actual data is as expected the case of n = 3 with a tapered horizontal velocity boundary condition. We note that a uniform velocity boundary condition results in a distinctly different and unrealistic profile of surface displacements.

The FE model results in Fig. 6 reflect the continuum deformation of the permafrost that dominates the relief extending from the polygon center to the proximal side of shoulders bordering the peripheral

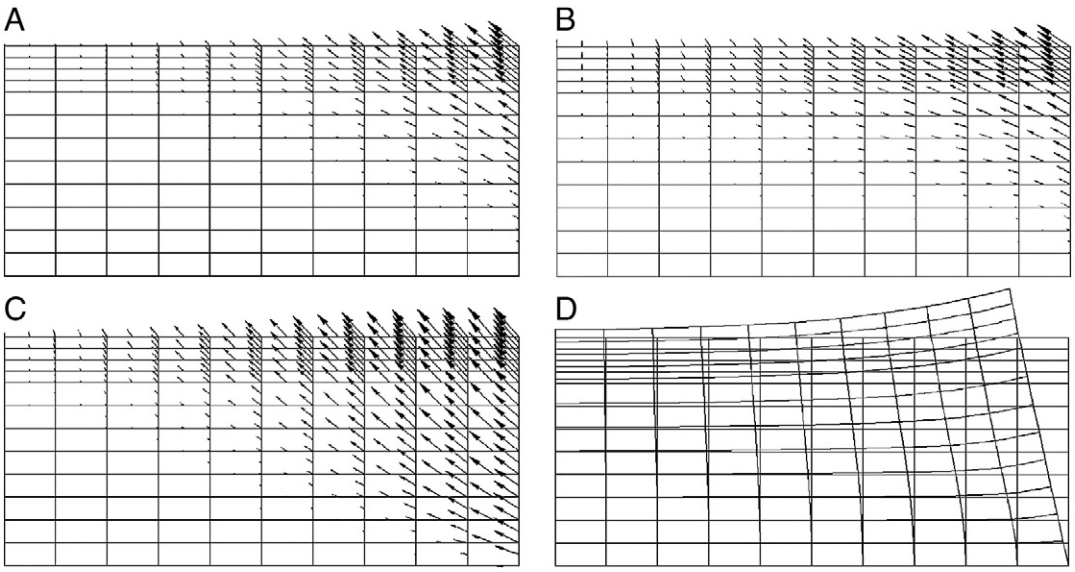


Figure 5. FEM modeling results. Upper figures illustrate the velocity field for the relatively realistic tapered horizontal velocity boundary condition for d = 0.5 mm a^{-1} at the surface, and different stress exponents in the flow law, $n = 3$ (A) and $n = 1$ (B). C results from specifying $n = 3$ and a uniform horizontal velocity boundary condition, 0.25 mm a^{-1}; it shows more broadly distributed deformation. D shows the typical undeformed and deformed FEM 2-D axi-symmetric mesh used in the model.

https://doi.org/10.1016/j.yqres.2010.12.009 Published online by Cambridge University Press

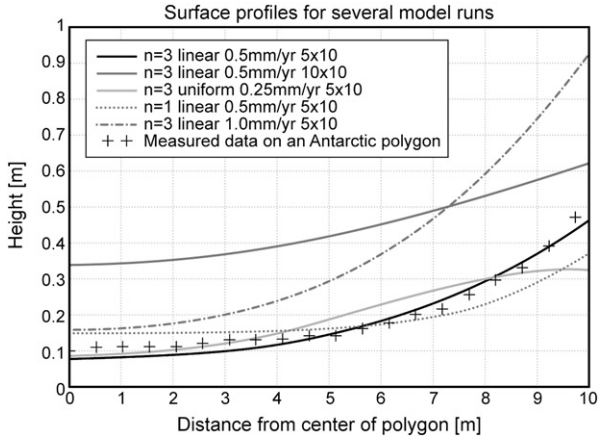


Figure 6. Calculated surface profiles for a range of boundary conditions and rheological models, assuming that calculated vertical velocities at the surface due to permafrost deformation are maintained through time. For comparison, we show a measured profile (crosses) across the shoulder of a representative polygon in Victoria Valley, Antarctica due to the growth of a sand wedge on the right side. According to the models the entire surface is also raised due to material input on the polygon sides; even the center of the polygon (at x = 0; left hand side) rises 0.1 m for the most realistic run.

contraction cracks. Fig. 7 illustrates the relief evolution due to this permafrost deformation combined with the downslope raveling (creep) of loose surface sand toward open cracks. For these results, the imposed horizontal velocity on the vertical side of the polygon decreases from 0.2 mm yr^{-1} at the surface, a representative value consistent with measurements of long-term divergence across cracks (Sletten et al., 2003) to 0 at 5 m depth. Values for the other model parameters were the power law exponent $n = 3$; transport rate coefficient for the surface creep K, 4×10^{-4} m^2 yr^{-1}; $S_c = 0.4$; and density, 2.4×10^3 kg m^{-3}. The figure shows the progressive growth of the conspicuous rounded shoulder with one half of the trough composed of the steeper, more planar slope extending to the contraction cracks (on left side); the other half of the trough, which is not shown, would be a mirror image. This slope is a distinct consequence of the creep law used (Eq. (2)); near the crack the inclination approaches S_c, typically within 10%. If instead of Eq. (2) the flux of sand is simply assumed to increase linearly with inclination, all parts of the shoulder are more rounded, no planar slope appears, and the maximum slopes are considerably steeper. In fact they would

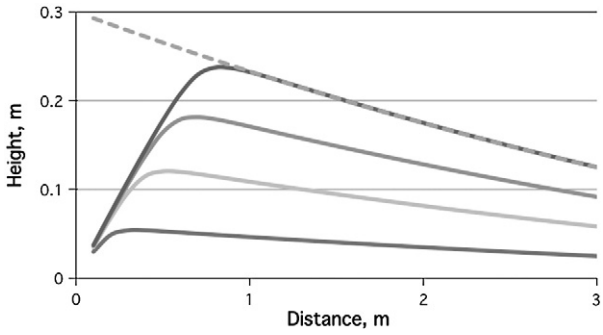


Figure 7. Computed surface profile of edge of polygon at four time intervals increasing up to 1500 yr (from lower to upper curves). The dashed curve shows the surface evolution without the downslope creep (raveling) of the loose sand. The contraction crack is on left side at $x \approx 0$; the center of the polygon is to the right at x = 10 m. The scaling factor for the velocity (Eq. 4), u_o, was set to 0.55 mm yr^{-1}, corresponding to a maximum rate of surface uplift of 0.2 mm yr^{-1}. The transport coefficient $K = 4\times10^{-4}$ m^2 yr^{-1}, and $S_c = 0.4$.

become unrealistic steep, as they would exceed the angle of repose of the loose surface material.

Discussion

Model idealization

We now consider the idealizations utilized in the model. The imposed horizontal velocity boundary conditions are reasonable given the inferred geometry of sand wedges, but much more data on sand-wedge geometry and orientation would be needed to refine or gain confidence in using this boundary condition.

Treating the ice-cemented permafrost as a non-linear material with creep properties similar to those of ice is appropriate as the permanent deformation surely involves ice deformation. On the other hand, skepticism is justified regarding the use of data on the downslope transport of loose sand in experimental sand piles that are subjected to vibrations as a basis for the treatment of the transport of granular material lacking ice cement near the surface of sand-wedge polygons. Although the experimental vibrations are clearly artificial, equivalent vibrations may well arise intermittently in the surface layer of loose sand in nature when it is subjected to powerful wind gusts, which are common in the Dry Valleys. These are known to dislodge and move surface grains up to 5 mm in diameter as seen in repeat photos, and the general mobility of surface grains is also evident from the rapid "healing" of surface disturbances (Putkonen, J., personal communication, 2010). The tempo of downslope surficial transport of loose material on the sand-wedge polygons is represented by a constant (K in Eq. 2). As the inclination of the ground surface decreases, K approaches the more widely known parameter, the topographic diffusivity, κ ($q = \kappa S$), which is useful in a number of ways. It permits comparison with other work on the surficial transport of granular material in the Dry Valleys and elsewhere, enables us to validate the parameter used in the granular creep model, and facilitates discussion of scaling issues.

The transport coefficient, K, used to generate the results in Fig. 7 corresponds to a topographic diffusivity of 4×10^{-4} m^2 yr^{-1} for low slopes. Interestingly, this value, which was chosen because it yielded realistic ground surface profiles, also appears reasonable as it is consistent with the upper portion of the range of topographic diffusivities (10^{-4} to 10^{-5} m^2 yr^{-1}) reported for diverse surfaces in the Dry Valleys by Putkonen et al. (2007) on the basis of repeat photographs, soil traps, and pebble transport distances. Much lower values of K yield ground-surface profiles for the polygon shoulders that show unrealistically sharp crests. As in all diffusive systems the intrinsic time scale, t, is linked to the system's length scale, l: $t = l^2/\kappa$. Here, for polygon shoulders 2 to 4 m wide and the diffusivity used above, t ranges from 1×10^4 to 4×10^4 yr. One implication of this result, which we explore next, is the evolution and longevity of the polygon relief once sand-wedge growth ceases. Such cessation would occur if the thermal contraction cracks are not refilled because, for example, wind-blown sand ceases to be available or entry into cracks becomes blocked because they become plugged or sealed by snow or coarse debris.

Surface reflection of sand-wedge growth and stability

Patterned ground marked by polygons with distinct shoulders bordering steep-sided troughs centered on contraction cracks indicates that sand wedges are growing actively. Without such growth, the permafrost deformation and uplift of the permafrost surface vanish, and the borders tend to smear out diffusively. Figure 8 shows how the relief developed in Figure 7 tends to degrade once wedges cease to grow. The shoulder flattens with time, the distance between the crest of adjacent shoulders increases, and all slopes become gentler. This relaxation of the relief illustrated in Figure 8

https://doi.org/10.1016/j.yqres.2010.12.009 Published online by Cambridge University Press

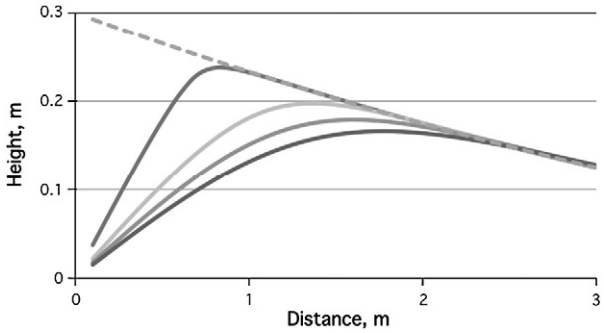


Figure 8. Degradation of shoulder once the sand wedge stops growing, starting with the end stage (upper curve) of the shoulder growth shown in Fig. 7 and ending after 9000 yr (lower curve). Three snapshots in time, equally spaced are shown. Model parameters are identical to those for Fig. 8 except that the uplift function, $u(x)$, has been set to zero.

occurs in 9000 yr, consistent with the intrinsic time scale (t) for this diffusive system, as just discussed.

More generally, the micro relief reflects the competition between the growth of shoulders forced by the widening wedges of sand and the diffusive relaxation due to surface creep of loose material. High, sharp shoulders reflect either active sand-wedging or slow creep. In contrast, polygons with little or no relief would suggest inactivity, unless they formed recently and the relief has not yet developed.

Caveats

Observation of actively widening wedges, as measured from Black's markers, and modeling results showing significant material motion at depth within the polygon, suggest that polygonal patterned ground activity in the Dry Valleys can pervasively deform the top several meters of the ground. Crack shifting in time, which has recently been documented experimentally in other contraction crack systems (e.g., Goehring et al., 2010), would lead to additional disturbance.

The model results are, however, sensitively dependent on the horizontal velocity field imposed to accommodate the growth of sand wedges, and hence are sensitive to the inferred wedge geometry. The work to date focuses on a simple wedge geometry, but this idealization may not be adequate in general because the actual geometry of sand wedges is poorly known as natural exposures are few and wedges are seldom excavated deeply and examined in detail. If for example, sand preferentially accumulated in the upper ~1 m of open cracks and seldom dribbled down to the lower portion of a wedge because of constrictions in the narrow crack, the sand wedges would tend to flare out near the surface. The corresponding deformation field in the permafrost accommodating such wedges would tend to be more localized and would not reach as deeply as for the wedges modeled herein (see Fig. 5). Taking into account the warming during the summer and the associated relatively large reduction in effective viscosity of the near the surface permafrost would also tend to increase the deformation close to the ground surface. This effect merits close attention because surface-parallel compressive stresses most likely arise and shoulder up the material on the sides of contraction cracks during the summer when the warming of the permafrost causes polygon expansion, which forces closure of the cracks; this results in shouldering and subsurface permafrost deformation as full closure is prevented by new debris that entered the cracks.

Comparison with long-term displacement field in ice-wedge polygons

We are optimistic that our numerical study will shed light on the pattern of long-term deformation of permafrost surrounding growing wedges, which is clearly evident in practically all exposure of ice wedges. The upturning of horizontal strata adjacent to wedges is consistent with the computed deformation field resulting from the growth of the wedge. Mackay (2000) and Mackay and Burn (2002) have documented in detail the long-term displacement patterns in the upper ~1 m of permafrost and the active layer in patterned ground areas and across single ice wedges. In his exhaustive and unprecedented study, Mackay (2000) derived long-term data for Garry Island on western Arctic coast in diverse complementary ways that revealed relative displacements at various depth. Collectively, they "demonstrate that there is a small net summer movement of the active layer outward from the stable polygon centers towards the ice-wedge troughs, independent of crack frequency." Moreover, in the long term, the polygon surface rises relative to the ice wedge based on multi-year measurements of the vertical position of pipes installed into the shallow permafrost and direct observations in an excavation showing that "that the frozen mud on both sides of the ice wedge had moved upward relative to the ice wedge" (Mackay and Burn, 2002).

These observations of net relative rise of the polygon surface, outward motion near the surface and ice-wedge growth, combined with our model results, suggest a relatively simple velocity field consisting of localized downwelling at the polygon edge and dispersed upwelling in the polygon interior, linked with radially outward motion in both the active layer and shallow permafrost, and slower motion of the permafrost toward the polygon center at depth. For sand-wedge polygons this downwelling is extremely localized and occurs as materials falls nearly vertically into the cracks at the polygon boundaries. The overall motion is a form of circulation in the upper few meters of permafrost and the active layer; an apt term would be wedge-induced cryoturbation. Interestingly it shares considerable similarity in terms of the kinematics and plan form with the classical Rayleigh–Benard convection cells, and yet arises from entirely different driving forces.

Europa's paired ridges

The shouldered edges of sand-wedge polygons separated by a conspicuous trough may well constitute an instructive terrestrial analog for geometrically similar features occurring on a much larger scale in a distant world. Paired ridges with a deep intervening trough are conspicuous and ubiquitous on the icy surface of Europa, one of the moons of the planet Jupiter (Fig. 9). They may indicate where the crust has pulled apart and at times allowed material from beneath the surface to well up and fill the cracks. Interestingly, one of the several

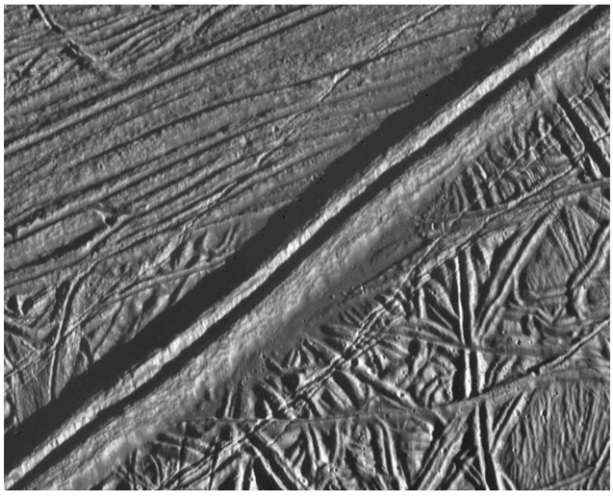


Figure 9. This view (PIA00589) of the icy surface of Jupiter's moon, Europa, shows paired ridges approximately 2.6 km wide and 300 m high. Transverse topographic profiles of these ridges closely resemble profiles across peripheral ridges on adjacent polygons (see Fig. 1). Image Credit: NASA/JPL/ASU.

https://doi.org/10.1016/j.yqres.2010.12.009 Published online by Cambridge University Press

hypothesis for the formation of these troughed double ridges developed by Turtle et al. (1998) is that they are "the surface expression of the intrusion of a narrow vertical dike beneath the ridge axis.... The ridge height is controlled by the amount of material intruded." In addition to the similarity in geometric form between the shouldered edges of polygons and Europa's paired ridges, both phenomena have been subject to similar numerical studies. The Europa problem has been approached through 2D finite element models of the deformation of ice caused by "moving the dike boundary away from the ridge [or center of the dike] at a specified rate" (Turtle et al., 1998) or "incremental ice-wedging" (Melosh and Turtle, 2004). The most recent work on ridge formation on Europa also uses numerical simulations to examine Europan ridge formation; it shows that "a pre-existing fracture zone promotes upwelling and lithospheric thinning, leading to topographic uplift of 50 m" (Han and Showman, 2008). However, a key feature of these fractures, the central trough flanked by identical ridges, is not reproduced in the simulations that lack incremental wedging.

Despite the similarity in the form of the paired ridges on Europa and those on sand-wedge polygons, the substantial differences in the size, materials, and general settings of these ridges, as well as the non-linearity of the flow law, call for caution in comparing the systems. For example, gravitational stresses, which are insignificant for the polygon micro-relief, would be much larger for the relief on Europa as it is two orders of magnitude larger, but this is partially offset by one order-of-magnitude lower gravitational force on Europa. Moreover, viscous stresses may still overwhelm gravitational stresses on Europa because its surface is much colder than the Antarctic (averaging −160°C), which makes the ice there much more viscous than on Earth. The most robust implication of the work herein for the Europan ridges is likely that "incremental wedging" is a viable mechanism for forming paired ridges with dimensions and morphology that are sensitive indicators of the depth and geometry of the wedging.

Conclusions

The modeling is a useful tool for exploring how crack growth and infilling, as well as other near-surface processes, are reflected in the micro relief of polygonal patterned ground. It shows quantitatively how the growth of a sand wedge causes permafrost deformation and shoulders aside surficial material to form low-center polygonal patterned ground, with the polygon edges marked by a characteristic ridge pair with an intervening trough centered on the wedge. With the exception of a central domain in polygons that remains undisturbed over the long term, the deformation affects the upper few meters of permafrost of each polygon, and crack shifting can lead to additional pervasive disturbance. The work presented here has clear implications for features seen on other planets, including very similar patterned ground found on Mars; and geometrically and perhaps genetically similar, but much larger, features on the icy surface of Europa.

Acknowledgments

The senior authors, BH and RS, are grateful for the good fortune to have known Link Washburn as a close colleague and co-worker. He inspired, guided, and helped us in many, many ways ranging from his unfailing, deep interest in patterned ground and other intriguing landforms characteristics of cold regions, to his untiring efforts to describe precisely and clearly what he saw in nature or in the laboratory, as well as the findings of other researchers, worldwide. We also benefited from the warm friendship of both Link and Tahoe Washburn, and their generous hospitality, whether it was extended to us in Bellevue, Washington or at their research "camp" at Resolute, Northwest Territories. We wish to thank Mike Malin for alerting the National Science Foundation about the importance of maintaining Black's sites, Tom Carpenter for his help with some of the profile measurements, and last but not least, an anonymous, diligent reviewer for a multitude of constructive comments that led to substantial improvements in this manuscript. This work was sponsored grant from the National Science Foundation (OPP-9726139, OPP-0636998) and NASA (NNH05ZDA001N).

References

Andersland, O.B., Sayles Jr., F.H., Ladanyi, B., 1978. Mechanical properties of frozen ground. In: Andersland, O.B., Anderson, D.M. (Eds.), Geotechnical Engineering for Cold Regions. McGraw-Hill, New York, pp. 216–275.
Black, R.F., 1973. Growth of patterned ground in Victoria Land, Antarctica. Permafrost: Second North American Contribution. Natl. Acad. of Sci, Yakutsk, Siberia, pp. 193–203.
Black, R.F., Berg, T.E., 1963. Patterned ground in Antarctica. Proceeding: Permafrost International Conference, Publ., 1287. Nat. Acad. of Sci.-Nat, Res. Counc., Washington, D. C, pp. 121–128.
Bockheim, J.G., Kurz, M.D., Soule, S.A., Burke, A., 2009. Genesis of active sand-filled polygons in lower and central Beacon Valley, Antarctica. Permafrost and Periglacial Processes 20, 295–308.
Burn, C.R., 2004. A field perspective on modelling "single-ridge" ice-wedge polygons. Permafrost and Periglacial Processes 15 (1), 59–65.
Cuffey, K.M., Paterson, W.S.B., 2010. The physics of glaciers, 4th Edition. Elesevier Press. 693 pp.
Durham, W.B., Kirby, S.H., Stern, L.A., 1992. Effects of dispersed particulates on the rheology of water ice at planetary conditions. Journal of Geophysical Research 97, 20883–20897.
Goehring, L., Conroy, R., Akhter, A., Clegg, W.J., Routh, A.F., 2010. Evolution of mud-crack patterns during repeated drying cycles. Soft Matter. doi:10.1039/b922206e.
Han, L., Showman, A.P., 2008. Implications of shear heating and fracture zones for ridge formation on Europa. Geophysical Research Letters 35, L03202. doi:10.1029/2007GL031957.
Hobbs, P.V., 1974. Ice Physics. Clarendon Press, Oxford, U.K.
Jahn, A., 1975. Problems of the Periglacial Zone (Zagadnienia Strefy Peryglacjalnej). National Technical Information Service, Springfield VA 22161; PB-248 901. 134 pp.
Kelly, M., Denton, G., Hall, B., 2002. Late Cenozoic paleoenvironment in southern Victoria Land, Antarctica, based on a polar glaciolacustrine deposit in western Victoria Valley. Geological Society of America, Bulletin 114, 605–618.
Kirby, S.H., Durham, W.B., Beeman, M.L., Heard, H.C., Daley, M.A., 1987. Inelastic properties of ice Ih at low temperatures and high pressures. Journal de Physiologie C1, 227–232.
Lachenbruch, A.H., 1962. Mechanics of thermal contraction cracks and ice-wedge polygons in permafrost. Geological Society of America Special Paper 70.
Lachenbruch, A.H., 1963. Contraction theory of ice-wedge polygons: a qualitative discussion. Proceeding: Permafrost International Conference. Nat., Acad. Sci.-Nat. Res. Counc., Washington, D. C, pp. 63–71.
Lefort, A., Russell, P.S., Thomas, N., McEwen, A.S., Dundas, C.M., Kirk, R.L., 2009. Observations of periglacial landforms in Utopia Planitia with the High Resolution Imaging Science Experiment (HiRISE). Journal of Geophysical Research 114 E04005 http://dx.doi.org/10.1029/2008JE003264.
Levy, J.S., Head, James W., Marchant, D.R., 2009a. Cold and dry processes in the Martian Arctic: geomorphic observations at the Phoenix landing site and comparisons with terrestrial cold desert landforms. Geophysical Research Letters 36 L21203 http://dx.doi.org/10.1029/2009GL040634.
Levy, J.S., Head, James W., Marchant, D.R., 2009b. Thermal contraction crack polygons on Mars: classification, distribution, and climate implications from HiRISE observations. Journal of Geophysical Research 114 E01007 http://dx.doi.org/10.1029/2008JE003273.
Mackay, J.R., 1971. The origin of massive icy beds in permafrost, western Arctic coast, Canada. Canadian Journal of Earth Sciences 8, 397–422.
Mackay, J.R., 1974. Ice-wedge cracks, Garry Island, Northwest Territories. Canadian Journal of Earth Sciences 11, 1366–1383.
Mackay, J.R., 1984. The direction of ice-wedge cracking in permafrost: downward or upward? Canadian Journal of Earth Sciences 21, 516–524.
Mackay, J.R., 1986. The first 7 years (1978–1985) of ice wedge growth, Illisarvik experimental drained lake site, western Arctic coast. Canadian Journal of Earth Sciences 23, 1782–1795.
Mackay, J.R., 1992. The frequency of ice-wedge cracking (1967–1987) at Garry Island, western Arctic coast, Canada. Canadian Journal of Earth Sciences 29, 236–248.
Mackay, J.R., 1993. The sound and speed of ice-wedge cracking, Arctic Canada. Canadian Journal of Earth Sciences 30, 509–518.
Mackay, J.R., 2000. Thermally induced movements in ice-wedge polygons, western arctic coast: a long-term study. Géographie Physique et Quaternaire 54, 41–68.
Mackay, J.R., Burn, C.R., 2002. The first 20 years (1978–1979 to 1998–1999) of ice-wedge growth at the Illisarvik experimental drained lake site, western Arctic coast, Canada. Canadian Journal of Earth Sciences 39, 95–111.
Matsuoka, N., 2011. Climate and material controls on periglacial soil processes: Toward improving periglacial climate indicators. Quaternary Research 75, 356–365.
Mellon, M., 1997. Small-scale polygonal features on Mars: seasonal thermal contraction cracks in permafrost. Journal of Geophysical Research 102, 25617–25628.
Mellon, M.T., Arvidson, R.E., Marlow, J.J., Phillips, R.J., Asphaug, E., 2008. Periglacial landforms at the Phoenix landing site and the northern plains of Mars. Journal of Geophysical Research 113. doi:10.1029/2007JE003039 E00A23.

https://doi.org/10.1016/j.yqres.2010.12.009 Published online by Cambridge University Press

Mellon, M.T., Malin, M.C., Arvidson, R.E., Searls, M.L., Sizemore, H.G., Heet, T.L., Lemmon, M.T., Keller, H.U., Marshall, J., 2009. The periglacial landscape at the Phoenix landing site. Journal of Geophysical Research 114. doi:10.1029/2009JE003418 E00E06.
Melosh, H.J., Turtle, E.P., 2004. Ridges on Europa: Origin by Incremental Ice-Wedging. Lunar Planet. Sci., XXXV, abstract 2029.
Nye, J.F., 1953. The flow law of ice from measurements in glacier tunnels, laboratory experiments and the Jungfraufirn borehole experiment. Proceedings of the Royal Society of London Series A 219 (1139), 477–489.
Pewe, T.L., 1959. Sand-wedge polygons (Tesselations) in the McMurdo Sound region, Antarctica — a progress report. American Journal of Science 257, 545–592.
Pewe, T.L., 1974. Geomorphic processes in polar deserts. In: Smiley, T.L., Zumberge, J.H. (Eds.), Polar Deserts and Modern Man. Univ. of Ariz. Press, Tucson.
Plug, L.J., Werner, B.T., 1998. A numerical model for the organization of ice-wedge networks. Permafrost Seventh International Conference Proceedings, pp. 897–902.
Plug, L.J., Werner, B.T., 2001. Fracture networks in frozen ground. Journal of Geophysical Research 106, 8599–8613.
Plug, L.J., Werner, B.T., 2002. Nonlinear dynamics of ice-wedge networks and resulting sensitivity to severe cooling events. Nature 17, 929–930.
Plug, L.J., Werner, B.T., 2008. Modelling of ice-wedge networks. Permafrost and Periglacial Processes. doi:10.1002/ppp. 604.
Putkonen, J., Rosales, M., Turpen, N., Morgan, D., Balco, G., Donaldson, M., 2007. Regolith transport in the Dry Valleys of Antarctica. In: Cooper, A.K., Raymond, C.R., et al. (Eds.), Antarctica: A Keystone in a Changing World — Online Proceedings of the 10th ISAES: USGS. Open-File Report 2007-1047, Short Research Paper, 103. doi:10.3133/of2007-1047.srp103. 5 pp.
Roering, J.J., Kirchner, J.W., Sklar, L.S., Dietrich, W.E., 2001. Experimental hillslope evolution by nonlinear creep and landsliding. Geology 29, 143–146.
Sletten, R.S., Hallet, B., Fletcher, R.C., 2003. Resurfacing time of terrestrial surfaces by the formation and maturation of polygonal patterned ground. Journal of Geophysical Research 108 (E4), 8044. doi:10.1029/2002JE001914.
Tsytovich, N.A., 1975. The Mechanics of Frozen Ground, Scripta. McGraw-Hill, New York.
Turtle, E.P., Melosh, H.J., Phillips, C.B., 1998. Tectonic modeling of the formation of Europan Ridges, (abstract). EOS, Transactions — American Geophysical Union 79 Suppl., F541.
Washburn, A.L., 1973. Periglacial Processes and Environments. Edward Arnold, London.
Weertman, J., 1983. Creep deformation of ice. Annual Review of Earth and Planetary Sciences 11, 214–240.

https://doi.org/10.1016/j.yqres.2010.12.009 Published online by Cambridge University Press